Supplementary Information

Table of content

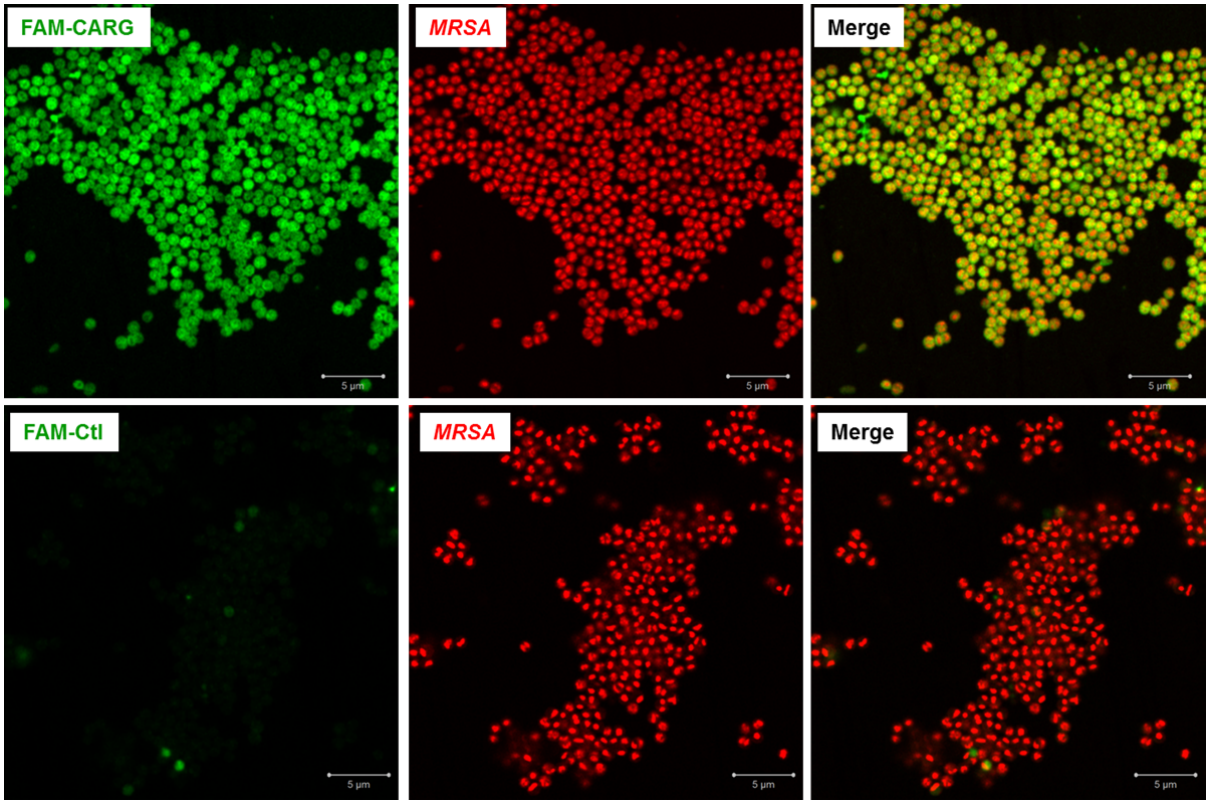

Figure S1. Selective binding of CARG peptide to a Methicillin-Resistant *S. aureus* (MRSA) strain in culture. Binding of FAM-labeled CARG peptide to the MRSA strain US300-0114 *in vitro* (top row). The control peptide (FAM-Ctl) shows no MRSA binding (bottom row). FAM-CARG or FAM-Ctl (green), bacteria nucleoids stained with DAPI (red). Scale bar: 5 µm

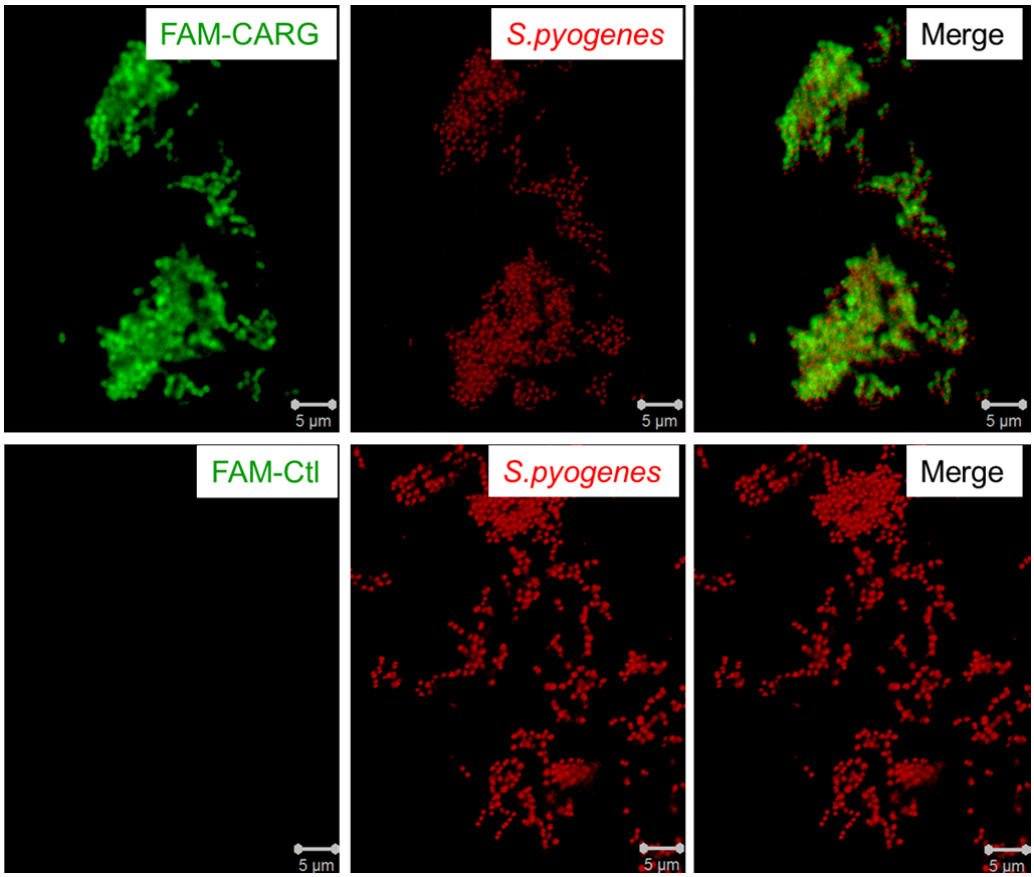

Figure S2. **Binding of CARG peptide to *Streptococcus pyogenes* strain in culture.** Binding of FAM-labeled CARG peptide to *S. pyogenes in vitro* (top row). The control peptide (FAM-Ctl) shows no Streptococcus binding (bottom row). FAM-CARG or FAM-Ctl (green), bacteria nucleoids stained with DAPI (red). Scale bar: 5 µm.

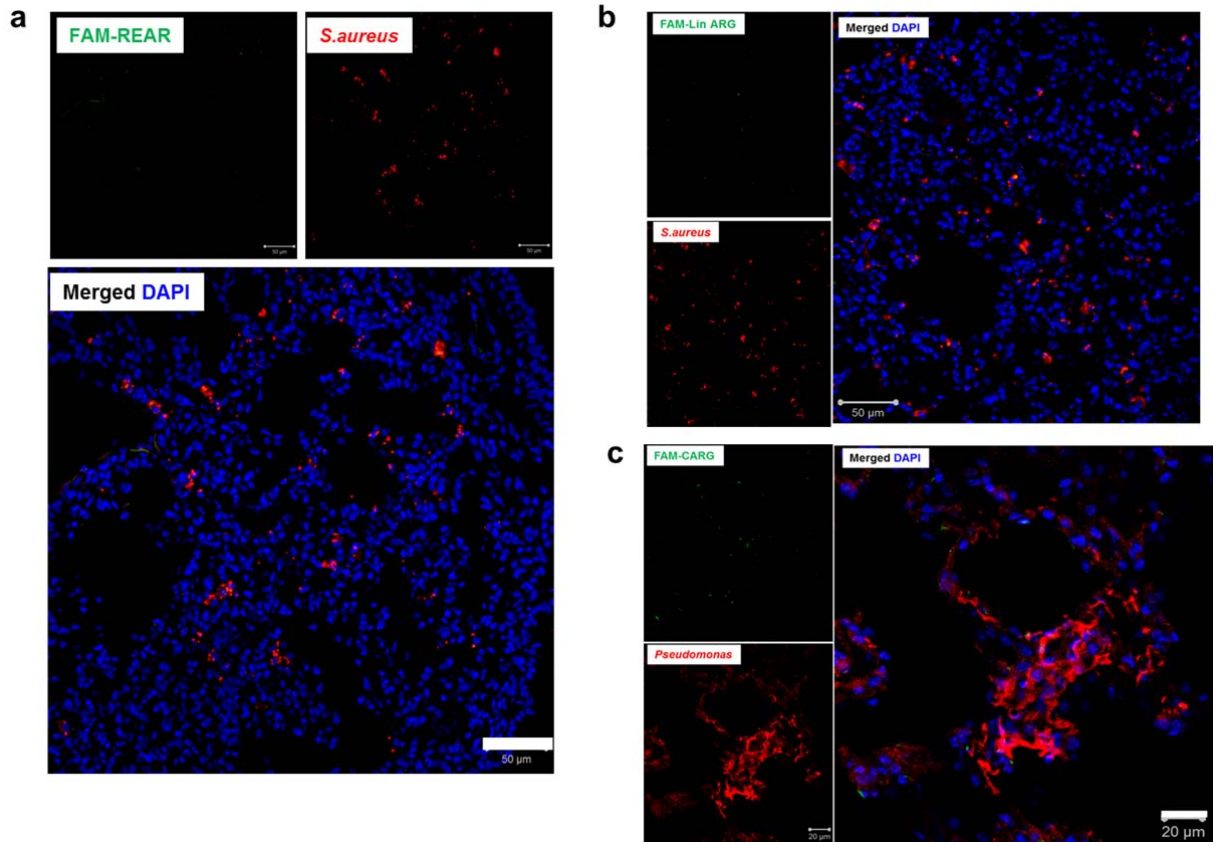

Figure S3. Control experiments establishing the high specificity of homing of the circular CARG peptide to *S. aureus* infected lungs. (a) Intravenously injected, FAM-labeled control peptide (CNREARGRC) does not home to *S. aureus*-infected lungs. FAM-peptide (FAM-REAR; green), Staphylococci (red), cell nuclei (blue). Scale bar: 50 µm (b) Intravenously injected FAM-labeled linearized version of CARG peptide (AARGGLKSA) does not home to *S. aureus*-infected lungs. FAM-peptide (green), Staphylococci (red), cell nuclei stained with DAPI (blue). Scale bar: 50 µm. (c) FAM-labeled CARG does not home to *P. aureginosa* infected lungs. *P. aeruginosa* pneumonia model was established by surgical inoculation of bacteria as described for the *S. aureus* pneumonia model. At 24 h post-infection, FAM-CARG was intravenously injected via tail vein and peptide presence in the lungs analyzed by confocal immunofluorescence microscopy. FAM-CARG (green), *P. aeruginosa* (red), cell nuclei (blue). Representative images of at least five *P. aeruginosa* infected lung sections (n = 3-5 mice) are shown. Scale bar: 20 µm. For comparison, data on homing of the cyclic CARG peptide to *S. aureus* infected lungs are given in Fig 4 of the main text and in Fig S5 below.

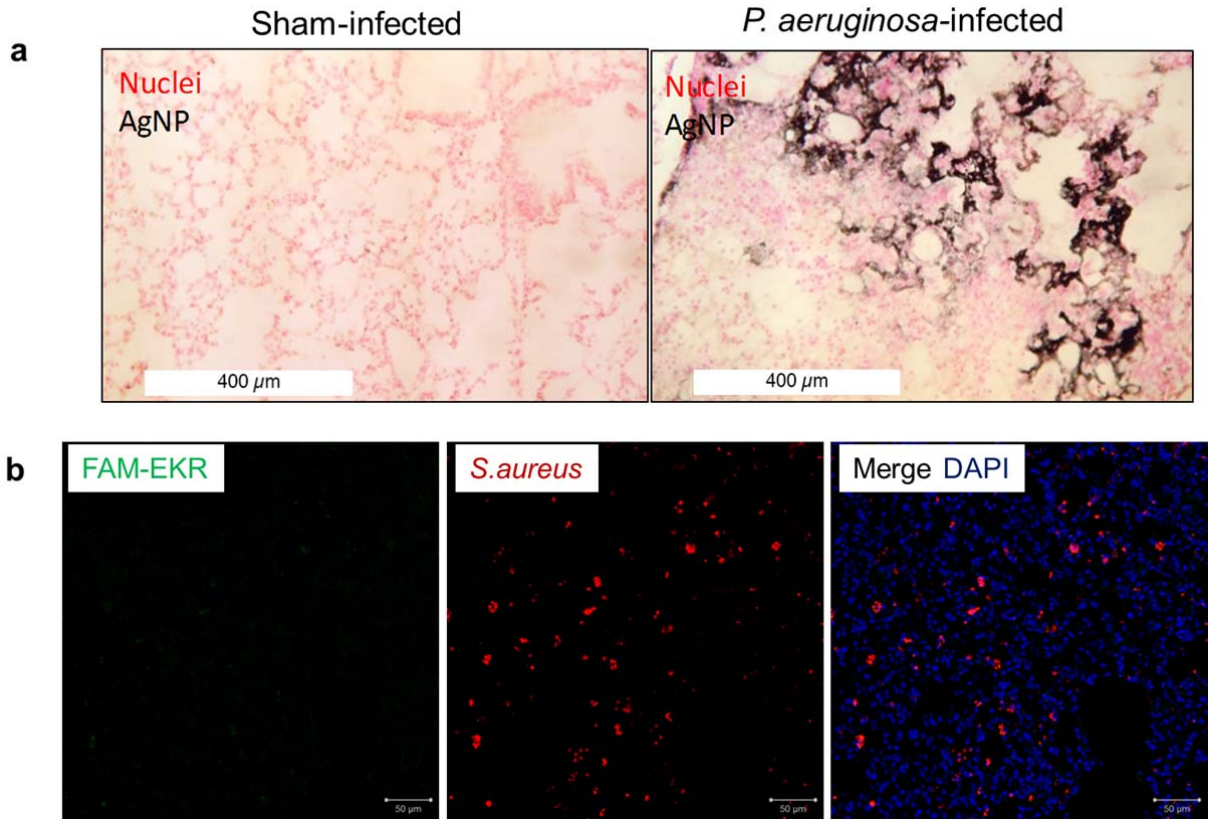

Figure S4: EKR peptide homes to *P. aeruginosa* but not to *S. aureus*-infected lungs. *P. aeruginosa* and *S. aureus* pneumonia models in mice were established by surgical inoculation of respective bacteria as described in the Materials and Methods section. (a) At 24 hours post-infection, mice with or without *P. aeruginosa*-induced lung infection were intravenously injected *via* tail vein with silver nanoparticles covalently conjugated with EKR-peptide (EKR-AgNP). After 1 h of circulation, the mice were terminally perfused with PBS and the lungs were excised, fixed in paraformaldehyde, and frozen for histological analysis. Serial sections stained with silver enhancement (Thermo Silver Enhancement Kit) plus Nuclear Fast Red counterstain showed intense accumulation of EKR-AgNPs in the regions of pseudomonas infection. No EKR-AgNP staining was detected in the lungs of a sham-infected mouse. (b) FAM-labeled EKR peptide does not home to *S. aureus*-infected lungs. At 48-72 h post-infection, FAM-EKR peptide was intravenously injected *via* tail vein and presence of the peptide in the lungs was analyzed by confocal immunofluorescence microscopy. FAM-EKR (green), *S. aureus* (red), cell nuclei (blue). Scale bar: 50 μm

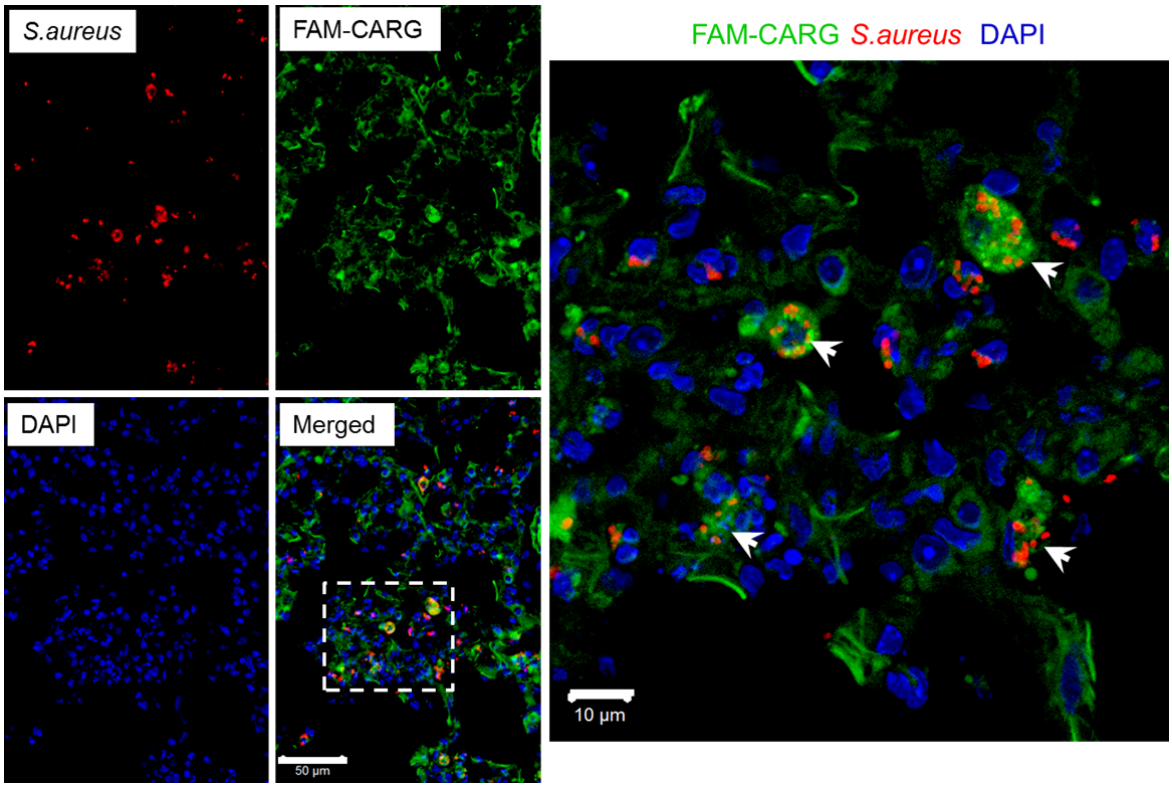

Figure S5. CARG peptide zeroes in on *S. aureus* bacteria at sites of infection and co-localizes with host phagocytic cells containing intracellular bacteria. The homing of FAM-labeled CARG to *S. aureus* infection was studied 24 hour post-infection. The FAM signal (green) shows strong homing and uptake in regions of *Staphylococcus*-infection (red). Cell nuclei are stained with DAPI (blue). The high magnification confocal image shows uptake and colocalization of the CARG peptide with engulfed bacteria in phagocytic cells (white arrows). Scale bar: 50 µm (low magnification) and 10 µm (high magnification).

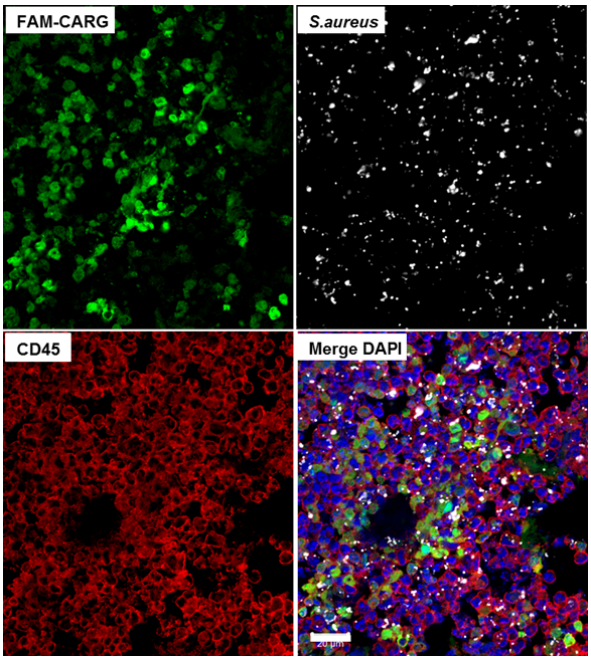

Figure S6. Homing and colocalization of CARG peptide to skin abscesses induced by *S. aureus*. Intravenously injected FAM-CARG peptide at sites of *S.aureus* skin infection and colocalization with host phagocytic cells. The FAM signal from the peptide (green) shows strong homing to regions containing Staphylococci (white, pseudocolor) and leukocytes (red). Cell nuclei, blue. Scale bar: 20 μm.

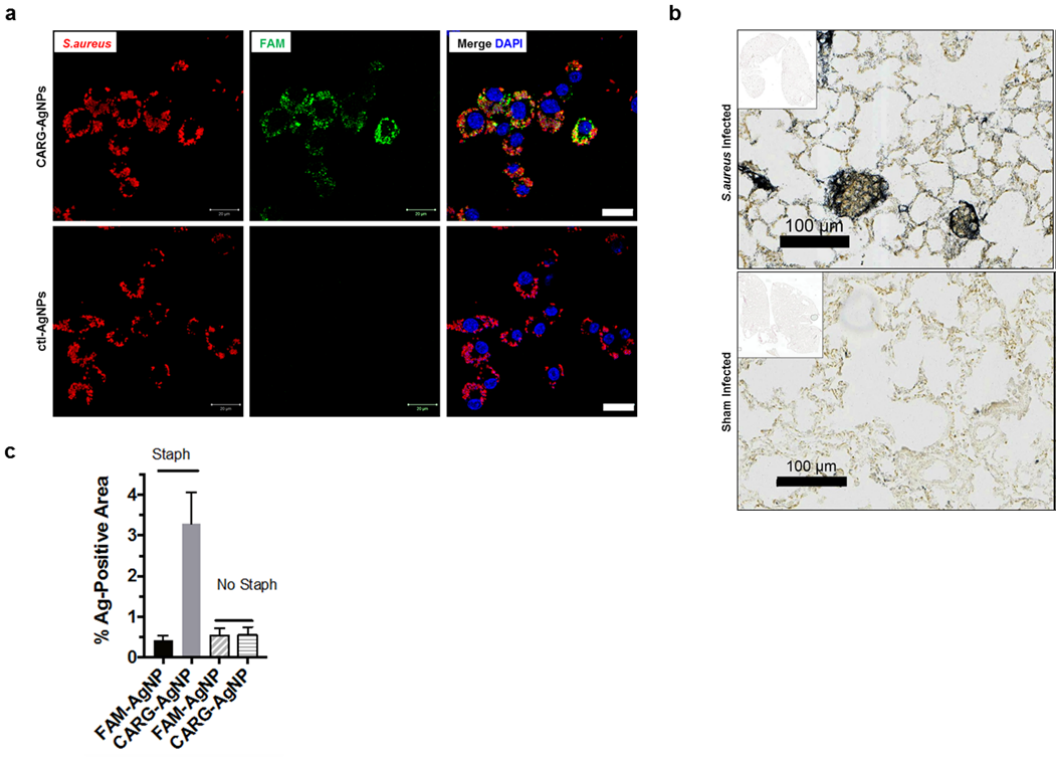

Figure S7. CARG mediated delivery of silver nanoparticles to *Staphylococcus*-infected cells *in vitro* and to lungs *in vivo*. (a) Silver nanoparticles were covalently conjugated with FAM-CARG peptide (CARG-AgNPs) or FAM control on the surface (Ctl-AgNPs). RAW 264.7 macrophages were incubated with *S. aureus* bacteria and the AGNPs. The binding and phagocytosis of bacteria-AgNP complexes was analyzed by confocal microscopy. (b) *S.aureus*-infected mice were intravenously injected with AgNPs 48-72 hours post-infection. After 1 h circulation, the mice were terminally perfused with PBS and the lungs were excised, fixed in paraformaldehyde and frozen for histological analysis. Lung sections were analyzed for silver (Ag) by immunohistochemistry. Scale: 100 µm. (c) Quantification of the Ag signal in infected and healthy lungs.

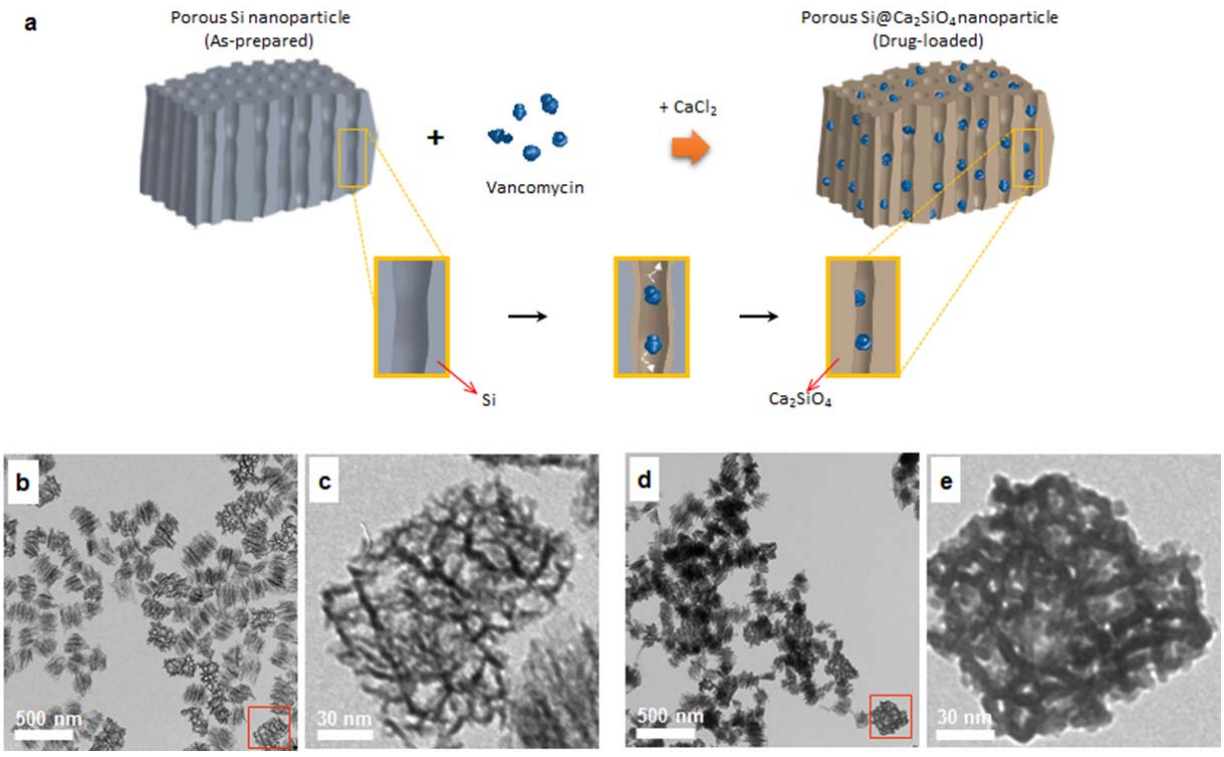

Figure S8. Self-sealing process to incorporate vancomycin to porous silicon nanoparticles (pSiNPs). (a) Schematic illustrations of the mechanistic steps involved in the self-sealing chemical reaction used to load the vancomycin payload. High concentration of calcium ions and vancomycin molecules freely diffuse into the pores, where calcium ions react with the locally high concentration of silicic acid released from silicon skeleton, resulting in formation of calcium silicate, which traps the vancomycin payload within the nanostructure. (b-e) Transmission electron microscope (TEM) images of (b and c) pSiNPs before vancomycin loading and (d and e) porous silicon-calcium silicate core-shell nanoparticles after the self-sealing process. As-prepared pSiNPs prior to calcium ion treatment show open porosity, whereas the drug-loaded nanoparticles display a more occluded porous structure with thickened pore walls, indicating the formation of a distinctive layer on the silicon skeleton upon reaction with calcium ions.

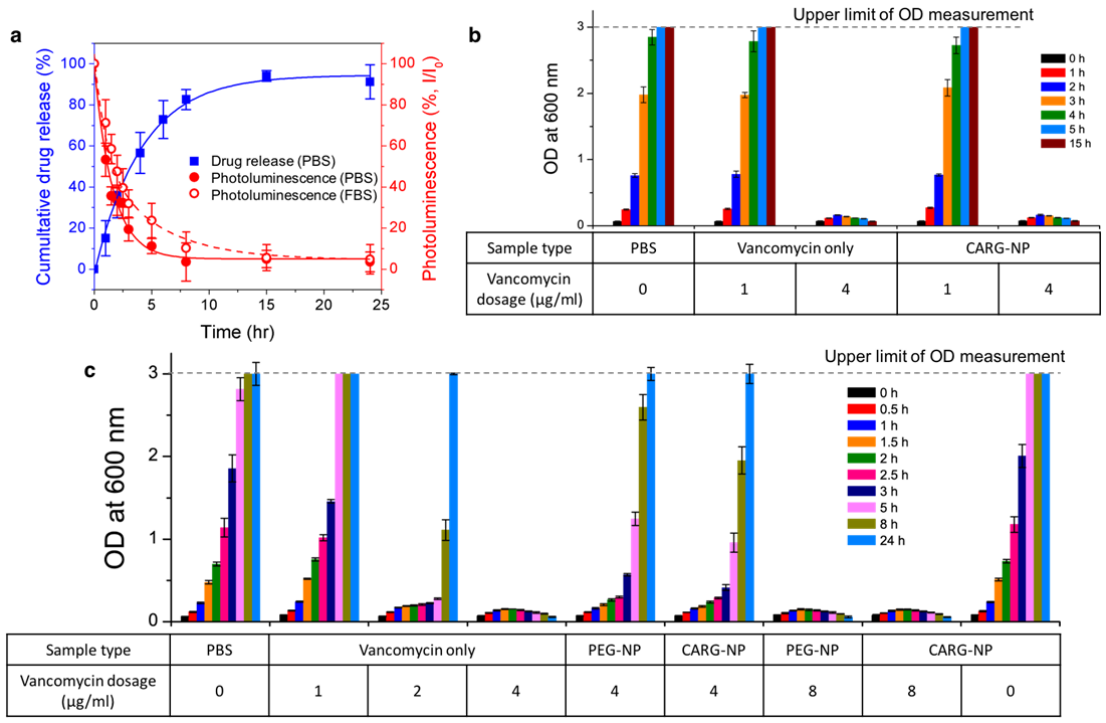

Figure S9. *In vitro* characterization of vancomycin-loaded nanoparticles. (a) Vancomycin release profile from pSiNPs prepared via self-sealing process and corresponding photoluminescence intensity. The readings were obtained from nanoparticles (50 μg/ml) incubated in phosphate-buffered saline (PBS) or fetal bovine serum (FBS) at 37 °C as a function of time. The pSiNPs were pelleted by centrifugation, and the absorbance of free vancomycin in the supernatant was measured at 280 nm. Photoluminescence spectra were measured with UV excitation (λ_{ex}: 365 nm), and emission intensities were integrated (λ_{em}: 550-950 nm) to generate the plot. Serum proteins interfered with the quantification (by optical absorbance) of vancomycin, but the degradation of the pSiNPs, was quantified by the loss of photoluminescence intensity intrinsic to the pSiNPs. Because the release of drug payloads from this type of formulation generally tracks pSiNP degradation,[1-3] the release of vancomycin was estimated from the change in photoluminescence intensity measured from the pSiNPs. The inferred vancomycin release was somewhat slower in FBS than in PBS; this is attributed to adsorbed serum proteins, as adsorbed proteins have been shown to slow the degradation/dissolution of porous Si.[4-6] However, it should be noted that the drug may be released via leaching, independent of pSiNP degradation, and so the inferred release rate may be an under-estimate of the actual rate of vancomycin release in FBS. (b) *In vitro* antibacterial activity of vancomycin released from vancomycin-loaded pSiNPs compared to pristine, free vancomycin, assessing the integrity of the antibiotic after it has been subjected to the chemistries associated with loading and release from the nanoparticles. In these experiments, vancomycin was loaded into the pSiNPs via the self-sealing process, the nanoparticles were conjugated to the CARG targeting peptide, and the resulting construct was incubated in PBS for 24h to release vancomycin from the particles as in (a). The supernatant was collected and then introduced into the culture tubes containing S. aureus in growth medium and the growth of *S. aureus* (optical density, OD) was monitored as a function of time. Plot shown in (b) represents measured OD at the indicated time points, for a PBS buffer control ("PBS"), free (as-received from the manufacturer) vancomycin ("Vancomycin only"), and vancomycin extracted from the nanoparticles as described above ("CARG-NP"). The dosage values reported along the x-axis correspond to the concentration of vancomycin in each culture tube. For the CARG-NP formulation, vancomycin concentration was determined assuming that all of the loaded vancomycin was released into the supernatant during the 24 h PBS incubation step. The data show that vancomycin released from the pSiNPs displayed the same potency as pristine vancomycin, establishing that the nanoparticle formulation chemistries and the

release process do not degrade the antibacterial properties of the vancomycin therapeutic. (c) *In vitro* antibacterial activity of the vancomycin-loaded pSiNPs compared to free vancomycin. In these experiments, the intact vancomycin-loaded pSiNPs were introduced directly into culture tubes containing *S. aureus* in growth medium, and the growth of *S. aureus* was quantified as a function of time. Plot shown in (c) represents measured OD at the indicated time points, for a PBS buffer control ("PBS"), free vancomycin from the manufacturer ("Vancomycin only"), vancomycin-loaded pSiNPs that contained an attached PEG linker but with no CARG targeting peptide (“PEG-NP”) and vancomycin-loaded pSiNPs that contained an attached PEG linker *and* attached CARG targeting peptide ("CARG-NP"). The dosage values reported along the x-axis correspond to the net concentration of vancomycin in each culture tube. The CARG-NPs showed a lower level of inhibition of bacterial growth compared to free vancomycin in this experiment. The weaker response of the CARG-NP formulation relative to free vancomycin here is attributed to the fact that drug is being released from the pSiNPs during the *S. aureus* incubation assay. This is consistent with the data from (a), which indicates that a lower concentration of free vancomycin is expected in the culture medium during the first 10-15 hours of the assay, as the nanoparticles required > 15 h to completely release their vancomycin payload under the experimental conditions. In contrast, vancomycin-loaded, CARG-coated pSiNPs were substantially more effective at killing bacteria than free vancomycin when tested *in vivo* (Figure 5 and 6 in main text). Empty pSiNPs showed no intrinsic antibacterial activity.

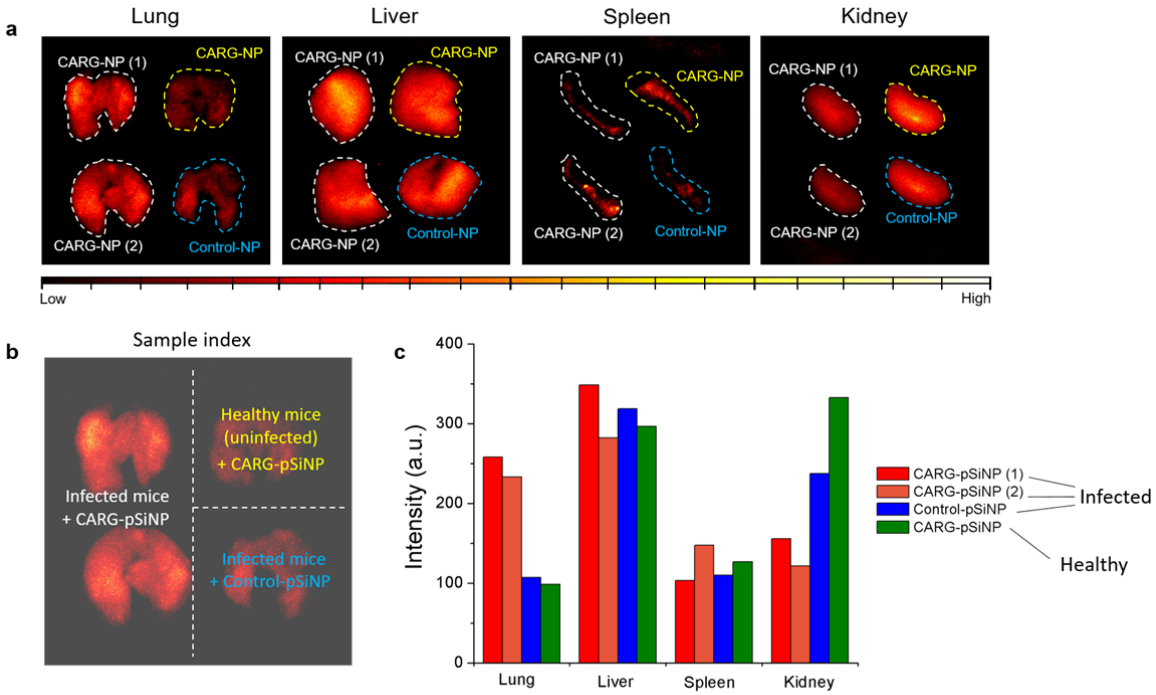

Figure S10. *In vivo* homing of CARG-coupled nanoparticles to infected lungs. Time-gated luminescence images show that accumulation of CARG-pSiNP in healthy lungs is similar to that of control nanoparticles (PEGylated pSiNP).

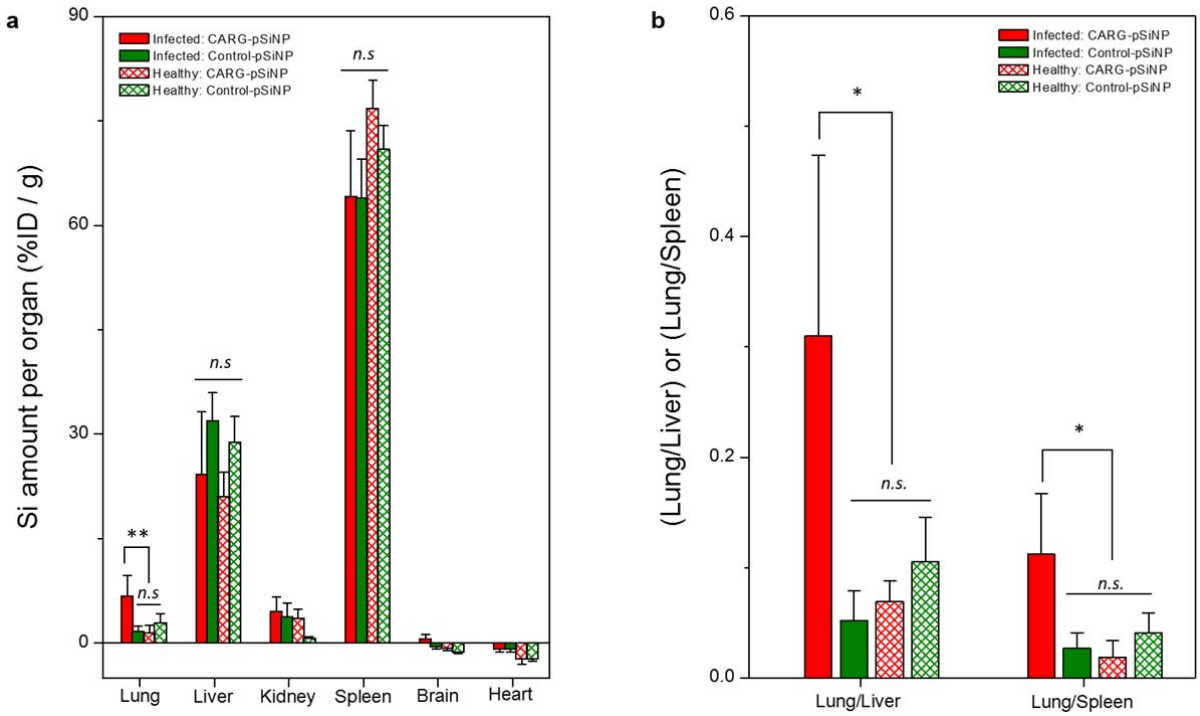

Figure S11. Biodistribution analysis of pSiNPs performed by ICP-OES. (a) Biodistribution profile of elemental silicon content in various organs in *S.aurerus*-infected and healthy mice. CARG-pSiNPs or Control-pSiNPs were allowed to circulate for 6 h and then the organs were harvested and analyzed by ICP-OES. The silicon content per organ is reported as the percent injected dose per gram (%ID/g), which is obtained by subtracting the endogenous background silicon present in tissues of control mice injected with PBS alone. (b) Accumulation of pSiNPs in the lung compared to liver and spleen, Data are expressed as the mean ± standard deviation, and the statistical analysis between experimental groups was obtained using the two-tailed Student's *t* test (n=4-5 per group; * $p < 0.05$, ** $p < 0.01$)

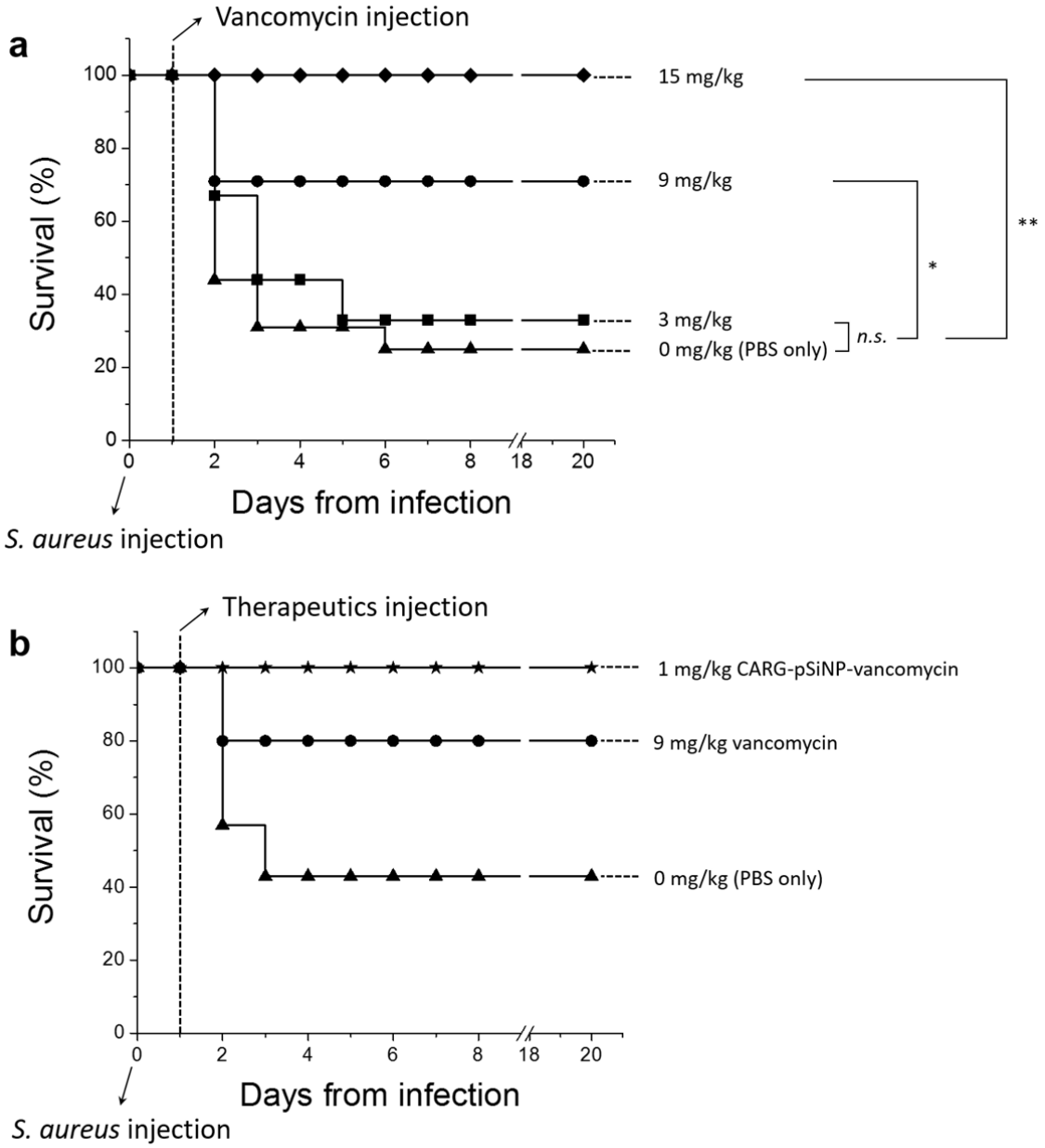

156

157 **Figure S12. Comparison of antibacterial efficacies of vancomycin delivered in CARG-pSiNPs and the**
158 **free drug in mouse *S. aureus* lung infection model.** (a) Kaplan-Meier survival analysis of mice treated with
159 different doses of free vancomycin administered as a single intravenous bolus 24 h post-infection (b) Survival
160 of lung-infected mice treated with different formulations of vancomycin, The infection and drug injections were
161 as in panel (a). Data analysis was performed using the statistical software GraphPad Prism (San Diego, CA,
162 USA ; n = 5-9; * $p < 0.05$; ** $p < 0.01$; *** $p < 0.001$; *n.s.*, not significant).

163

164

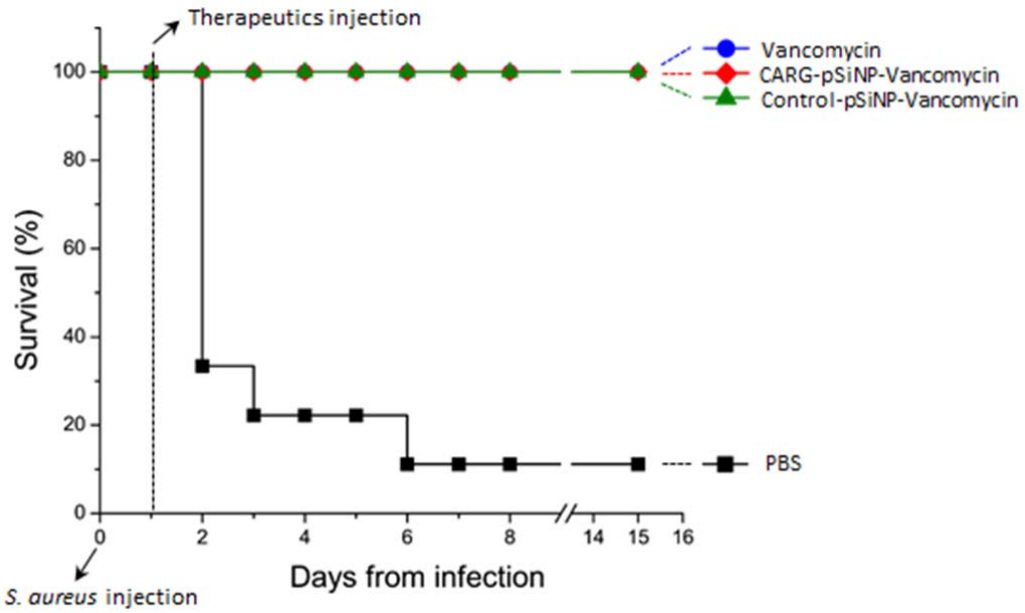

Figure S13. *In vivo* survival rate of mice treated with high dosage of vancomycin. All mice recovered from *S aureus* lung infection, when15 mg/kg of vancomycin whether as free or NP-incorporated drug was used. (*n* = 9 mice for PBS group; *n* = 3 mice/group for the other treatments).

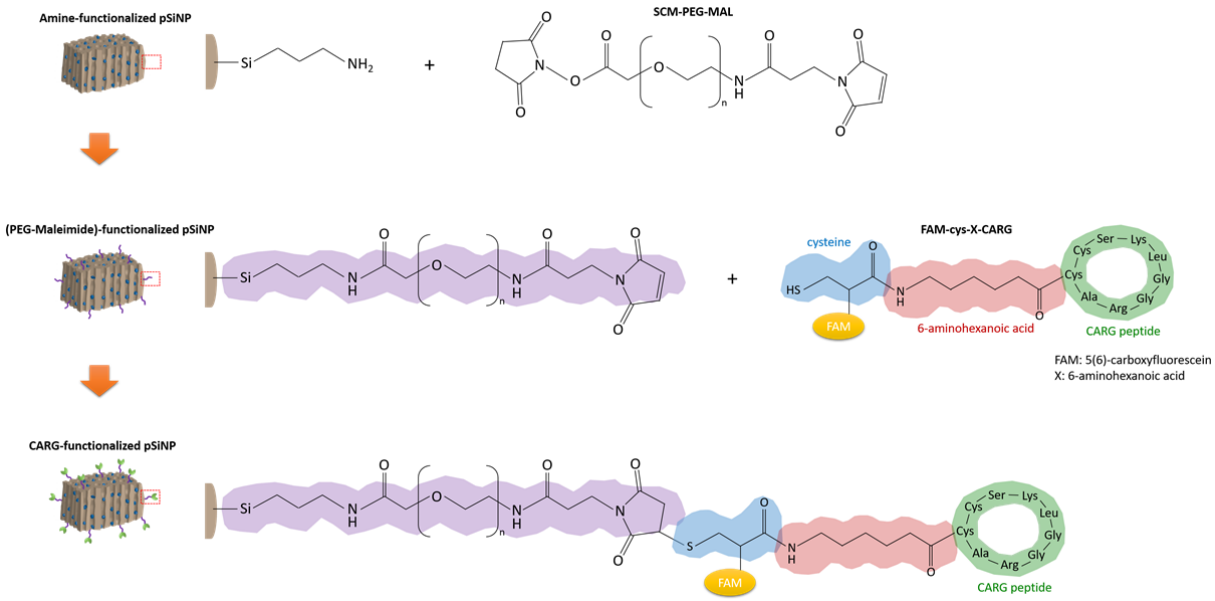

Figure S14. Schematic illustration depicting the chemical structure of the CARG peptide and its grafting to pSiNPs. The CARG peptide consists of a cyclic 9-amino acid sequence with a 6-aminohexanoic acid spacer and free cysteine at the N-terminus. The free cysteine is labeled with 5(6)-carboxyfluorescein (FAM), and further conjugated to a maleimide group on the pSiNP.

Table S1: Effect of CARG-targeted or non-targeted pSiNPs loaded with vancomycin on the activities of serum liver enzymes in mice.

Groups	Serum ALT [‡] (U/L)	Serum AST [%] (U/L)
CARG-pSiNP-Vancomycin	135.3 ± 48.32	242.3 ± 28.81
Control-pSiNP-Vancomycin	122 ± 74.38	128 ± 36.61
Free Vancomycin	115.7 ± 41.03	256 ± 60.48

Male Balb/c mice (n=3 per group) were injected intravenously with 3 mg/kg of vancomycin, either loaded in pSiNP or as free drug. After 24 hours, blood was collected and analyzed for liver enzymes. The results expressed as the means ± SEM.

Abbreviations: AST, Aspartate Aminotransferase; ALT, Alanine Transaminase.

[‡] Reference intervals in male Balb/c mice; age 8-10 weeks: 28-132 U/L.

[%] Reference intervals in male Balb/c mice; age 8-10 weeks: 55-352 U/L

References

1. Park, J.-H. et al. Biodegradable luminescent porous silicon nanoparticles for in vivo applications. *Nature Mater.* **8**, 331-336 (2009).

2. Joo, J. et al. Porous Silicon-Graphene Oxide Core-Shell Nanoparticles for Targeted Delivery of siRNA to the Injured Brain. *Nanoscale Horiz.* **1**, 407-414 (2016).

3. Kang, J. et al. Self-Sealing Porous Silicon-Calcium Silicate Core–Shell Nanoparticles for Targeted siRNA Delivery to the Injured Brain. *Adv. Mater.* **28**, 7962-7969 (2016).

4. Perelman, L.A., Pacholski, C., Li, Y.Y., VanNieuwenzhe, M.S. & Sailor, M.J. pH-Triggered Release of Vancomycin from Protein-Capped Porous Silicon Films. *Nanomedicine* **3**, 31-43 (2008).

5. Orosco, M.M., Pacholski, C., Miskelly, G.M. & Sailor, M.J. Protein-coated porous silicon photonic crystals for amplified optical detection of protease activity. *Adv. Mater.* **18**, 1393-1396 (2006).

6. Dancil, K.-P.S., Greiner, D.P. & Sailor, M.J. A porous silicon optical biosensor: detection of reversible binding of IgG to a protein A-modified surface. *J. Am. Chem. Soc.* **121**, 7925-7930 (1999).